

Chitosan-Guar Gum Coated SCOBY Bacterial Cellulose As A Potential Material For Sustainable Wound Dressing

Kayla Kenenza¹, Alexandra A Wihardja¹, Kyu H. Cho¹, Rajratna Ramteke^{*2}, Karinina Putri¹, and Ros Maria Andesko¹, Savita Sondhi¹

¹BINUS SCHOOL Simprug, Kota Jakarta Selatan, Daerah Khusus Ibukota Jakarta 12220, Indonesia

²Government Medical Colledge Bhandara, 441 904, India

Corresponding author: Rajratna Ramteke (rajratnaramteke@gmail.com)

Abstract: The prevalence of wounds, antimicrobial resistance, and medical waste calls for development in the field of wound care, including the creation of an eco-friendly dressing which is able to speed up wound healing through moisture retention and antimicrobial activity. This study aims to create a potential wound dressing material containing bacterial cellulose from a kombucha pellicle, coated with chitosan (CH) and guar gum (GG). CH and GG were coated at varying ratios (70:30, 50:50, 30:70) and then tested for chemical composition, mechanical strength, swelling capacity, and antimicrobial activity. Fourier Transform Infrared (FTIR) and Raman spectroscopy confirmed successful coating with CH and GG. SC-CH-GG (30:70) showed highest tensile strength. While SC-CH-GG (70:30) showed enhanced swelling capacity (908.26% ± 150.31%) and inhibited *Staphylococcus aureus* (12.5 mm) making a potential alternative dressing material in the treatment of chronic wounds.

1. INTRODUCTION

Breaks in the skin, commonly caused by burns, accidents, and disease are known as wounds as described by (Saxena et al, 2024 and Gobi et al, 2021). Once the skin is compromised, it is vulnerable to infection by microorganisms as stated by Mie et al, (2018). The ideal wound dressing should be inexpensive, accessible, provide physical protection against external contaminants, absorb excess exudate, and have sufficient mechanical strength and antimicrobial properties (Gardikiotis et al, 2022 and Bano et al, 2017). Although dressings traditionally used in clinical settings are inexpensive and provide protection from external contaminants, they cannot maintain a moist wound environment as reported by Ghomi et al, (2019).

The spread of multidrug-resistant bacteria as highlighted by Prasilyanto et al, (2024), coupled with the environmental concerns arising from overuse of synthetic polymers noted by Gupta et al, (2025), establishes a need for modern wound dressings which retain moisture and contain inherent antimicrobial activity. Consequently, as per Gobi et al, (2021) natural polymers such as bacterial cellulose (BC) which are biocompatible and biodegradable, have gained attention for their potential in the wound dressing application. Further, BC has demonstrated greater water absorption and mechanical stress in comparison to vegetable cellulose, making it an attractive prospect for wound dressings, according to Laavanya et al, (2021). Symbiotic Culture of Bacteria and Yeast (SCOBY) is produced during kombucha tea fermentation and contains BC. SCOBY is originally used to start the next batch of fermentation or is discarded, but now it is being explored to exploit the properties of its BC composition. The addition of other materials is used to complement the swelling capacity and tensile strength of SCOBY BC, tailoring it for the wound dressing application. Márquez-Reyes et al, (2022) previously combined SCOBY BC with chitosan to explore its antimicrobial and antioxidant properties. SCOBY BC coated with chitosan and hydrolyzed collagen has also been explored in relation to antimicrobial activity, mechanical property, and drug loading/releasing performance reported by Yakaew et al, (2022). However, there is a need to focus the exploration on enhancing SCOBY BC's moisture retention, while still producing sufficient tensile strength and antimicrobial activity through the incorporation of other materials.

As a derivative of chitin, chitosan's cationic nature makes it favorable in the wound dressing application, due to being intrinsically antimicrobial and biodegradable noted by Bano et al, (2017). Chitosan is also abundant and low cost, produced as waste from the seafood industry outlined by Singh et al, (2017). Meanwhile, guar

gum is a natural polymer which is easily producible, low cost, and renewable - obtained from the endosperm of *Cyamopsis tetragonolobus* characterized by Sharma et al, (2018) The combination of chitosan and guar gum are well-studied and reported an improvement on tensile strength, antimicrobial activity, and fluid uptake (Rahman et al, 2021; Hong et al, 2024 and Barman et al, 2024).

This study uses BC from SCOBY with chitosan and guar gum to produce a simple, low cost, and eco-friendly patch with increased swelling capacity to accelerate wound healing. SCOBY is first purified and then coated with chitosan and guar gum. The patches were then assessed by FTIR analysis and Raman imaging for chemical characterization, and for tensile strength, elasticity, swelling capacity and antimicrobial activity.

2. Experimental

2.1 Materials

Chitosan powder that has a degree of deacetylation >70% was supplied by Bio Chitosan Indonesia, while guar gum was purchased from Mitra Jaya Chemicals Ltd. The SCOBY was acquired from a local market in Indonesia.

2.2 Purification of SCOBY

The purification process was done as described by Amarasekara et al, (2020), with minor modifications. The SCOBY was washed in distilled water, patted dry, then placed in 1.0M NaOH twice over a period of 2 h at 90°C. It was again rinsed using distilled water, dried, and treated with 1.5 NaOH overnight. Lastly, the SCOBY was dried in the oven at 55°C.

2.3 Preparation of Patches

Chitosan (CH) was added to 0.1M acetic acid while guar gum (GG) is dissolved in distilled water to create a 2% CH solution and 2% GG solution, respectively. Purified SCOBY is then dipped into 100 g of a mixture containing different CH-to-GG ratios for 5 min followed by air drying at room temperature.

The patches created are SCOBY only (SC), SCOBY with chitosan (SC-CH), as well as SCOBY with chitosan and guar gum (SC-CH-GG) at CH:GG ratios 70:30, 50:50, and 30:70.

2.4 Chemical Characterization

The patches were submitted to Universitas Indonesia for Fourier Transform Infrared (FTIR) analysis and Raman spectroscopy. The FTIR was conducted using the Shimadzu IRXross Mode ATR-diamond crystal FTIR spectrophotometer with a range of 4000 to 400 cm^{-1} and a resolution of 4 cm^{-1} . Raman spectroscopy analysis was conducted using the Horiba/LabRam Odyssey with a spatial resolution in the order of 0.5-1 μm .

2.5 Swelling

To identify the amount of fluid that the patches can hold, 10x10mm patches were immersed in 37°C phosphate buffer saline (PBS). The patches were removed at set time intervals, blotted with tissue paper, and then weighted (labelled W_f). Before conducting the test, the dry samples were weighted as well (labelled W_i). These values are substituted into Eq. (1) to determine the swelling capacity of the patch (%). A total of 3 trials were conducted on each patch.

$$\% \text{ of Swelling} = \frac{W_f - W_i}{W_i} \times 100\% \quad (1)$$

2.6 Antimicrobial Activity

Patches were first autoclaved at 121°C for 15 minutes and then sent to Qlab at Universitas Pancasila to assess antimicrobial activity against *Staphylococcus aureus* (*S. aureus*) and *Escherichia coli* (*E. coli*) via agar diffusion assay using 24-hour-old TSA media. One loop of the inoculum was mixed with sterile TSB and adjusted to a wavelength of 600 nm using UV-Vis spectroscopy. Then, 0.1 mL of the inoculum was spread evenly on the frozen agar where the sample was placed alongside chloramphenicol (30 μg) as a control group, and aerobically incubated at 37°C for 18-24 hours. The plates were then observed for clear zones indicating inhibition.

2.7 Mechanical Properties

The elasticity and tensile strength of the material was tested at BINUS Alam Sutera using an EZ Test Texture Analyzer (EZ-SX) with a 50N load cell. A total of 3 trials was conducted on each patch under standard laboratory conditions.

3. RESULTS

3.1 Physical Characterization

The process of creating the patches is shown in Fig. 1, while the final patches are displayed in Fig. 2. The initial SCOBY was moist with a light brown appearance, rubber-like texture and generally flat, variation in terms of smoothness and thickness was observed. These distinctions may be attributed to an uneven cellulose distribution and varying fibril size in the kombucha pellicle, as observed by Tran et al, (2021). After purification, the SCOBY turned white as a result of NaOCl treatment and had a paper-like texture due oven drying. From undergoing immersion in CH and GG, the dry SCOBY rehydrated and became more flexible. After coating and air drying, a higher CH concentration led to a browner color in the patch. The thickness of the final patches measured are within the range of 0.95 - 2.02 mm, as recorded in Table 1.

3.2 Chemical Characterization

The FTIR analysis ensured our method for preparing the patches were successful. The same technique of immersion was used for all CH:GG ratios, so SC-CH-GG (50:50) was selected as a representative for this analysis. The FTIR spectra overlay for SC-CH, SC, and CH are shown in Fig. 3a, while the overlay for SC-CH-GG, CH, and GG are shown in Fig. 3b. The FTIR spectrum for SC-CH shows an absorption band at 3275 cm^{-1} and 3327 cm^{-1} that overlap. This is similar to the FTIR spectrum for SC-CH-GG where there is an absorption band at 3296 cm^{-1} and 3348 cm^{-1} that overlap. These ranges indicate a stretching vibration of the O-H and N-H functional groups which are identical to the CH compound. Meanwhile, absorption of 750 cm^{-1} to 1250 cm^{-1} can be seen in SC-CH-GG only, which is identical to the GG compound. Lastly, the distinct peaks at 1000 cm^{-1} to 1100 cm^{-1} that are exhibited in both overlays indicates the presence of cellulose in the sample. The Raman spectra taken at 2 different points of the SC-CH-GG patch, are displayed in Fig. 4a and Fig. 4b. The results showed a distinct peak at 1100 cm^{-1} , which corresponds to the C-O stretching in polysaccharides and indicates the presence of cellulose. The peak falls within the 750 cm^{-1} to 1250 cm^{-1} range, where the FTIR detected an absorption band characteristic of GG. Thus, SC-CH-GG patches produced in this study can be recognized as containing CH and GG.

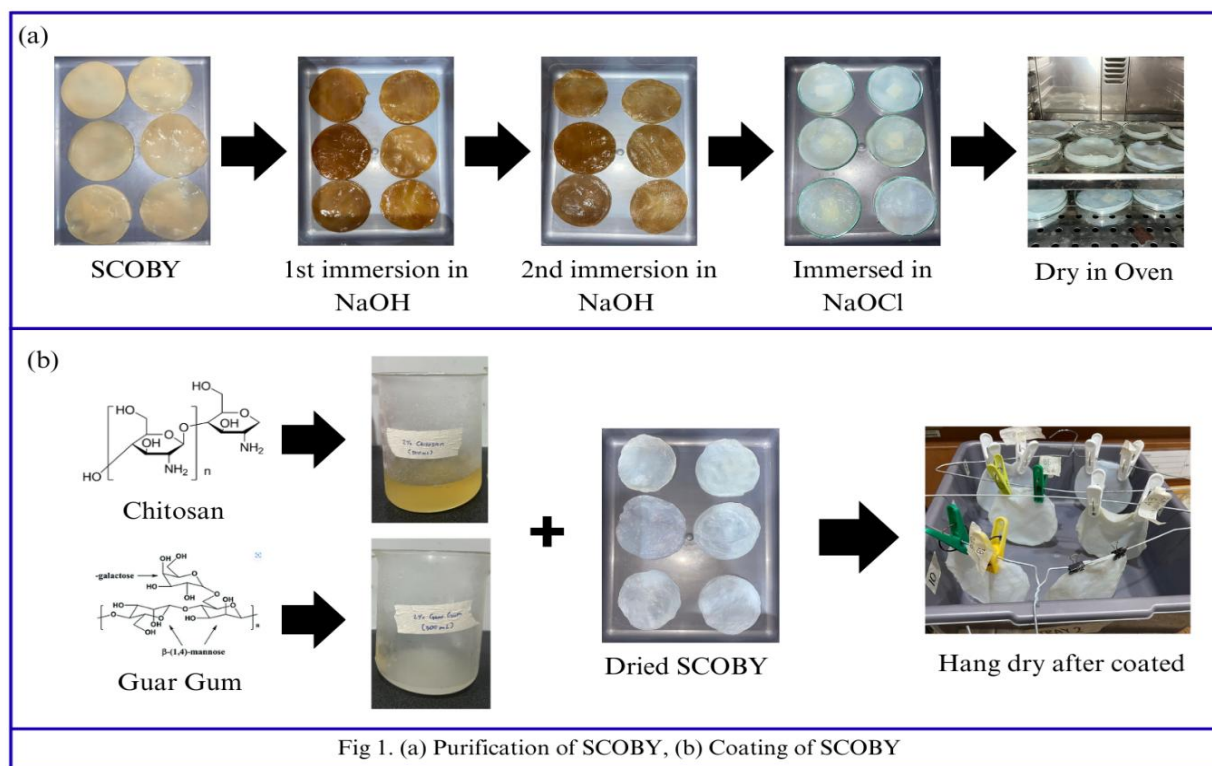


Fig 1. (a) Purification of SCOBY, (b) Coating of SCOBY

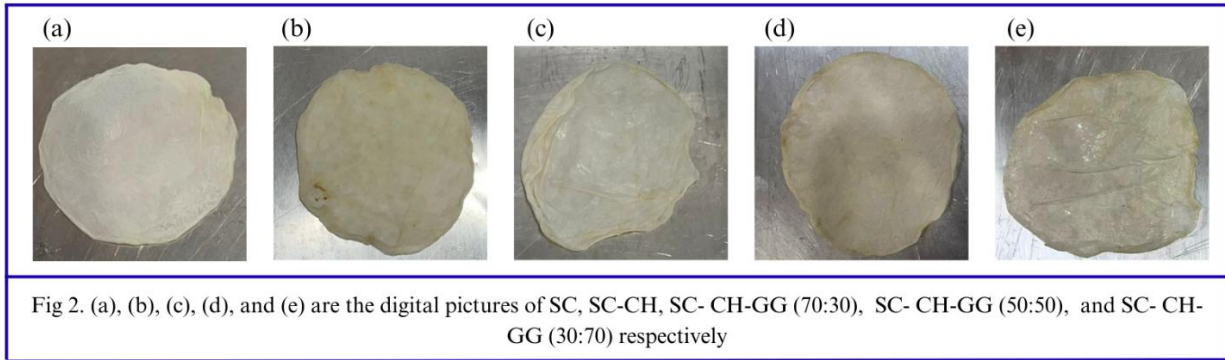
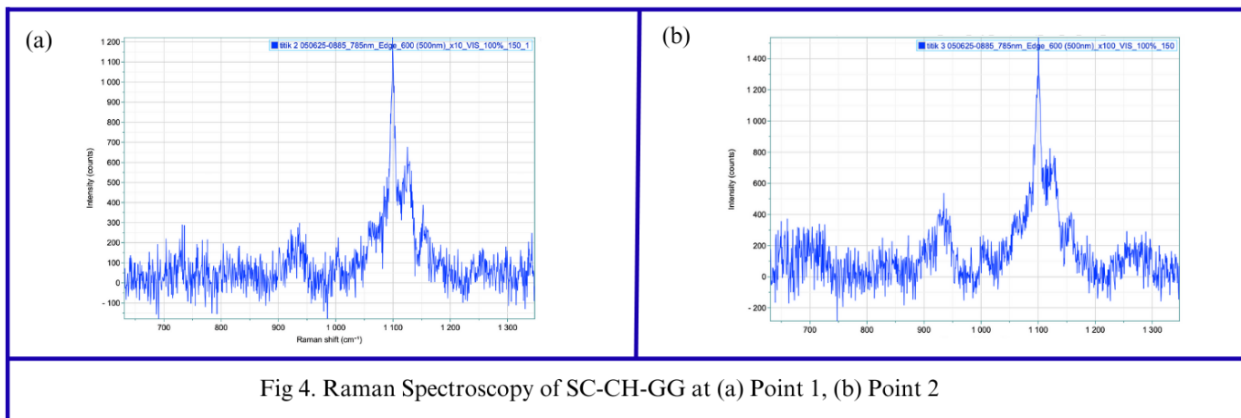
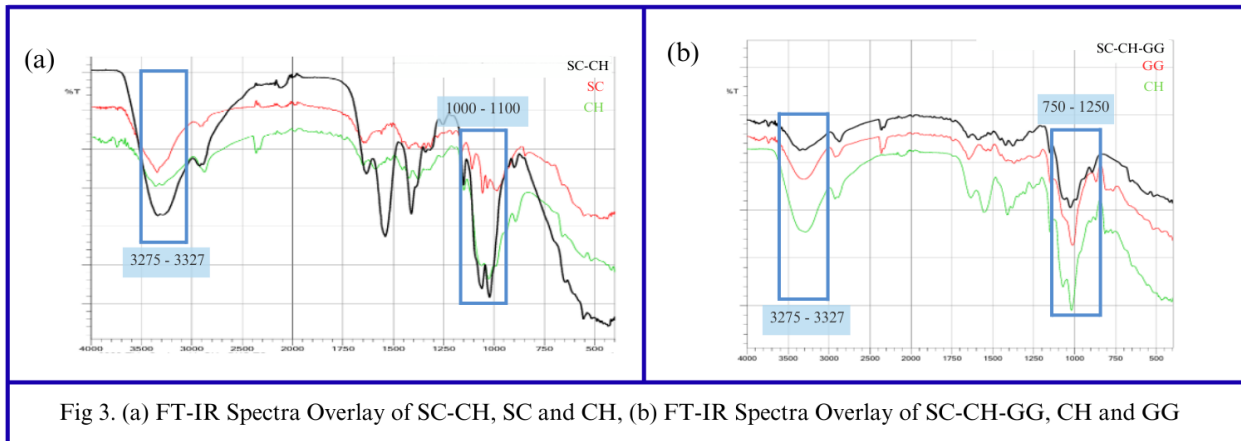


Table 1. Thickness of Patches

No.	Type	Thickness (mm)
1	SC	2.02 ± 2.62
2	SC-CH	1.22 ± 0.25
3	SC-CH-GG (70:30)	1.58 ± 0.43
4	SC-CH-GG (50:50)	0.95 ± 0.70
5	SC-CH-GG (30:70)	1.03 ± 0.48



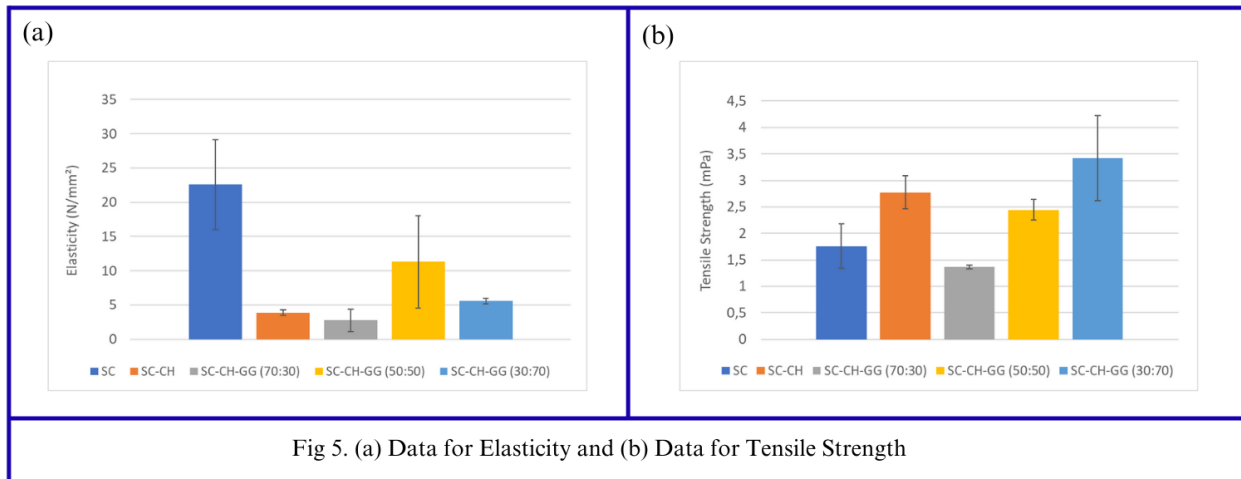


Fig 5. (a) Data for Elasticity and (b) Data for Tensile Strength

3.3 Mechanical Properties

The elasticity and tensile strength (TS) of patches produced are presented in Fig. 5a and Fig. 5b, respectively. SC recorded the highest elasticity value at $22.58 \pm 6.53 \text{ N/mm}^2$. When CH is added, there is a decrease in elasticity as seen in SC-CH ($3.90 \pm 0.40 \text{ N/mm}^2$). By blending GG into the SC-CH patches, it created different effects depending on the CH:GG ratio. A ratio with lower GG content (70:30) resulted in an even further decrease in elasticity ($2.78 \pm 1.63 \text{ N/mm}^2$). Meanwhile, a ratio with equal or higher GG content mixed into the SC-CH formulation resulted in increased elasticity. This is seen in the 50:50 and 30:70 ratio producing values of $11.31 \pm 6.74 \text{ N/mm}^2$ and $5.58 \pm 0.44 \text{ N/mm}^2$, respectively. SC achieved a TS of $1.76 \pm 0.42 \text{ mPa}$, which is increased by the addition of CH as shown in SC-CH ($2.78 \pm 0.32 \text{ mPa}$). Similar to elasticity, the ratio of GG content had varying effects on the TS recorded. The 30:70 ratio achieved the highest TS of $3.42 \pm 0.80 \text{ mPa}$, followed by the 50:50 ratio at $2.44 \pm 0.19 \text{ mPa}$, and the 70:30 ratio at $1.37 \pm 0.04 \text{ mPa}$.

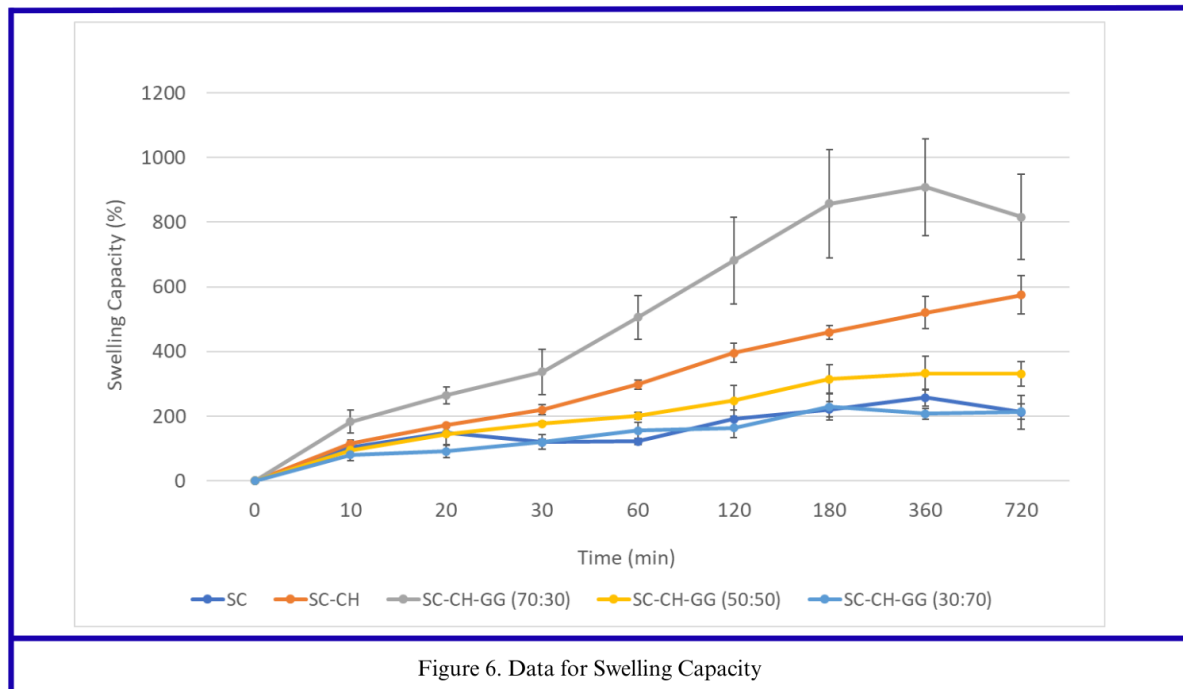


Figure 6. Data for Swelling Capacity

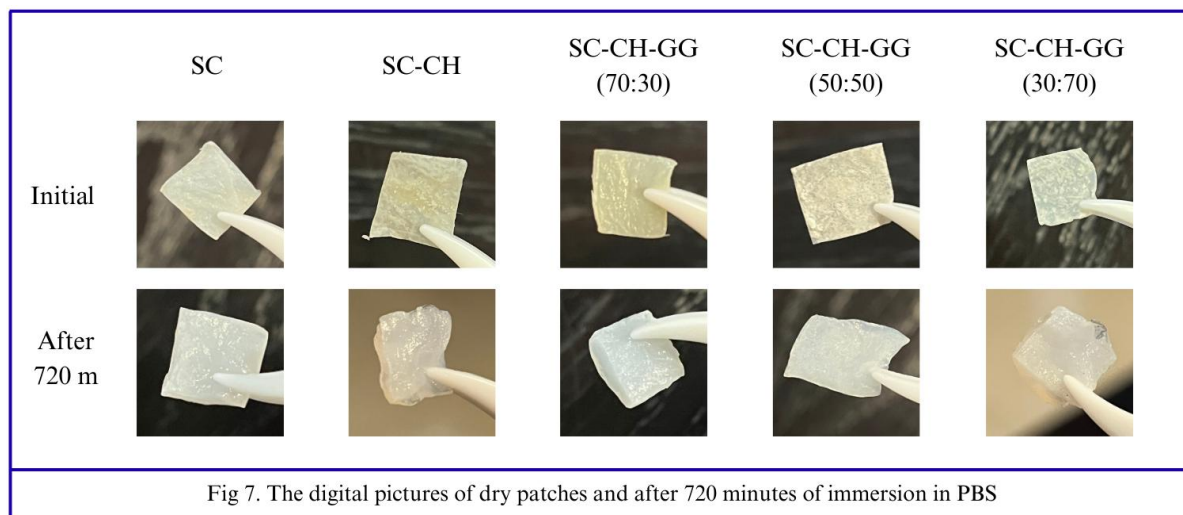


Fig 7. The digital pictures of dry patches and after 720 minutes of immersion in PBS

3.4 Swelling Capacity

The swelling capacity of the films over time are shown graphically in Fig. 6, and visually in Fig. 7. All patches except SC-CH had reached equilibrium by 360 minutes. Although SC-CH showed the second highest swelling capacity overall ($575.12\% \pm 59.28\%$), the patch became deformed after immersion in PBS solution. The incorporation of GG in certain ratios helped the patches retain more of their original shape, with the 70:30 ratio maintaining the most structural integrity. SC-CH-GG (70:30) displayed a significantly higher swelling capacity than all other patches ($908.26\% \pm 150.31\%$), supported by a visible increase in thickness. SC-CH-GG (50:50) was also able to maintain its original shape, reaching a maximum capacity of $332.47\% \pm 52.38\%$. SC and SC-CH-GG (30:70) produced similar values of $257\% \pm 25.81\%$ and $229.17\% \pm 41.35\%$ respectively, with the 30:70 ratio becoming slightly deformed.

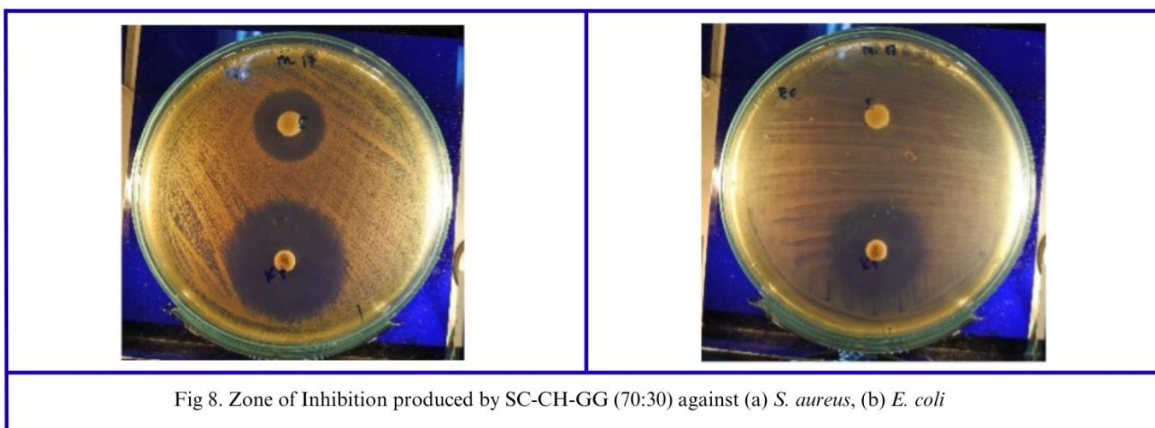


Fig 8. Zone of Inhibition produced by SC-CH-GG (70:30) against (a) *S. aureus*, (b) *E. coli*

3.5 Antimicrobial Properties

The agar diffusion assay was conducted in triplicates for each patch, with the average zone of inhibition (ZoI) calculated and assessed. SC-CH-GG (70:30) produced an inhibition zone of 12.5mm against *S. aureus*, but did not inhibit the growth of *E. coli* as seen in Fig. 8. Other formulations (SC, SC-CH, SC-CH-GG (50:50), SC-CH-GG (30:70) did not produce a zone for inhibition against *S. aureus* or *E. coli*.

4. DISCUSSION

The FTIR analysis and Raman spectroscopy was done to verify the presence of chemical compounds CH and GG in our formulated patches. The analysis displayed that both SC-CH and SC-CH-GG produced absorption

bands corresponding to pure CH. In addition, the SC-CH-GG showed absorption bands corresponding to pure GG. This verifies that our method of sample preparation was successful.

According to Safta et al, (2025), Wound dressings should contain adequate TS to avoid mechanical failure, while maintaining sufficient elasticity to maximize patient comfort. Among all compositions, SC-CH-GG (30:70) showed the greatest TS (3.42 ± 0.80 mPa). This indicates that an increased concentration of GG creates a stronger patch. A similar report was made by Barman et al, where the highest TS value was recorded at the 30:70 CH-to-GG ratio. Some of our results deviated from the findings of Rao et al, (2010), who reported that combinations of CH and GG often perform better than CH alone. The differences in result may be associated with slight variations in SCOBY thickness before purification, which influences its following mechanical properties, as noted by Daus et al, (2024). Meanwhile, SC produced the greatest elasticity value of 22.58 ± 6.53 N/mm² due to its naturally elastic character explained by A. Chong et al, (2024). The addition of CH significantly decreased elasticity in all formulations, due to CH's natural rigidity as a result of containing a dense hydrogen bond network, as described by M. Chen et al, (2018).

Dressings should also be able to absorb exudate from the wound site to decrease the likelihood of infection, which is especially important for the healing of chronic wounds, as noted by J. S. Mervis, (2025). The ability for exudate absorption was measured through swelling capacity. SC-CH-GG (70:30) displayed a significantly higher swelling capacity than the rest (>900%), likely due to the CH and GG blend forming an amorphous structure that enhances absorption, mentioned by Tshikovhi et al, (2025). This synergistic effect has been reported by Aneeqa Zarbab et al. (2023) and other studies, where blending of GG at low concentrations aids in maintaining moisture.

Although the structure formed by CH and GG at 70:30 increases swelling capacity, it simultaneously decreases TS. The inverse relationship between the two properties can be observed by the 70:30 ratio producing the lowest TS, while the 30:70 (highest TS) produced the lowest swelling capacity. SC-CH itself was able to produce the second highest TS and swelling capacity, however it could not maintain its structural integrity in the PBS solution. The lack of structural integrity in SC-CH may be attributed to non-uniformity in the absorption of liquid, due to its rigid structure.

To further reduce the risk of infection and ultimately facilitate rapid wound healing, dressings with intrinsic antimicrobial properties are favored. As purified SCOBY BC does not contain inherent antimicrobial properties, as reported by Dang et al, (2025), the SC patch did not develop an inhibition zone for both *S. aureus* and *E. coli*. CH, which has been widely reported to display antimicrobial activity by Bano et al, (2017), was added to SC to enhance our patch. However, as noted by Ardean et al. (2021), CH's antimicrobial activity is largely limited by its low aqueous solubility, which is likely the reason why our SC-CH formulation did not display any antimicrobial properties. By incorporating GG, SC-CH-GG (70:30) displayed clear antimicrobial activity against *S. aureus* (12.5mm inhibition zone). The 70:30 ratio with the highest swelling capacity is correlated in enhancing the antimicrobial activity of CH. Furthermore, the patch exhibited antimicrobial activity against *S. aureus* bacteria but not *E. coli*, since CH is more susceptible to gram-positive bacteria as per Ke et al, (2021). Conversely, higher concentrations of GG (50:50 and 30:70) did not show antimicrobial activity. Rao et al, (2020) also noted the decrease in antimicrobial activity with the addition of more GG in CH, suggesting hydrogen bonding between the (-OH) group of GG and NH₃⁺ in CH as the cause for this.

The SC-CH-GG patch developed at a 70:30 ratio displayed satisfactory properties, including high swelling capacity, and antimicrobial activity against *S. aureus*. Therefore, this makes it a promising material to support healing of the wound, especially for the treatment of chronic wounds that release large amounts of exudates and are prone to infection. However, further research must be conducted to improve the tensile strength and elasticity of the patch so that its efficacy as a dressing material is enhanced. In addition, detailed biological assessments are necessary to assess biocompatibility and its effect on the human body.

5. CONCLUSION

In this study, patches using SCOBY BC coated with chitosan and guar gum were developed successfully. Notably, the SC-CH-GG (70:30) patch displayed an enhanced ability to absorb wound exudate and inhibit

growth of *S. aureus*, making it suited towards treating chronic wounds. With the SC-CH-GG patches formulated from low-cost and biodegradable materials, it could potentially serve as an alternative to traditional wound dressings that are non-biodegradable.

Acknowledgements

The research described in this paper was financially supported by the IB Global Youth Action Fund 2025. Authors are grateful to the BINA NUSANTARA GROUP for providing support to conduct this research.

Conflict of Interest

The authors declare no conflict of interest

REFERENCES

- [1] S. Saxena et al., "Biomedical Materials for Sustainable Wound Care: A Review of Environmental Impact and Clinical Efficacy," *E3S Web of Conferences*, vol. 552, no. 01060, pp. -, July 2024, doi: 10.1051/e3sconf/202455201060
- [2] R. Gobi et al., "Biopolymer and Synthetic Polymer-Based Nanocomposites in Wound Dressing Applications: A Review" *Polymers*, vol. 13, no. 12, pp. 1962, June 2021, doi: 10.3390/polym13121962
- [3] M. Mie et al., "Synthetic polymeric biomaterials for wound healing: a review" *Progress in Biomaterials*, vol. 7, no. 1, pp. -, Feb. 2018, doi: <https://doi.org/10.1007/s40204-018-0083-4>
- [4] I. Gardikiotis et al., "Borrowing the Features of Biopolymers for Emerging Wound Healing Dressings: A Review" *Int. J. Mol. Sci.*, vol. 23, no. 15, pp. -, Aug. 2022, doi: 10.3390/ijms23158778
- [5] I. Bano et al., "Chitosan: A potential biopolymer for wound management", *Int. J. Bio. Macromolecules*, vol. 102, no. -, pp. 380-383, Sept. 2017, doi: <https://doi.org/10.1016/j.ijbiomac.2017.04.047>
- [6] E. R. Ghomi et al., "Wound dressings: Current advances and future directions", *J. App. Poly. Sci.*, vol. 236, no. 27, pp. -, July 2019, doi: <https://doi.org/10.1002/app.47738>
- [7] M. E. Prastiyanto, S. Darmawati, B. S. Daryono, and E. Retnaningrum, "Examining the prevalence and antimicrobial resistance profiles of multidrug-resistant bacterial isolates in wound infections from Indonesian patients," *Narra J*, vol. 4, no. 2, p. e980, Aug. 2024, doi: <https://doi.org/10.52225/narra.v4i2.980>.
- [8] M. N. Gupta et al., "Sustainable dressings for wound healing," *Biotechnology for Sustainable Materials*, vol. 2, no. 1, pp. -, Jan. 2025, doi: <https://doi.org/10.1186/s44316-024-00023-w>
- [9] D. Laavanya, S. Shirkole, and P. Balasubramanian, "Current challenges, applications and future perspectives of SCOBY cellulose of Kombucha fermentation," *Journal of Cleaner Production*, vol. 295, p. 126454, May 2021, doi: <https://doi.org/10.1016/j.jclepro.2021.126454>.
- [10] J. M. Márquez-Reyes et al., "Production and Characterization of Biocomposite Films of Bacterial Cellulose from Kombucha and Coated with Chitosan," *Polymers*, vol. 14, no. 17, p. 3632, Jan. 2022, doi: <https://doi.org/10.3390/polym14173632>.
- [11] P. Yakaew, T. Phetchara, P. Kampeerapappun, and K. Srikulkit, "Chitosan-Coated Bacterial Cellulose (BC)/Hydrolyzed Collagen Films and Their Ascorbic Acid Loading/Releasing Performance: A Utilization of BC Waste from Kombucha Tea Fermentation," *Polymers*, vol. 14, no. 21, p. 4544, Jan. 2022, doi: <https://doi.org/10.3390/polym14214544>.
- [12] R. Singh et al., "Chitin and chitosan: biopolymers for wound management," *Int. World J.*, vol. 14, no. 6, pp. 1276-1289, Aug. 2017, doi: 10.1111/iwj.12797
- [14] G Sharma et al., "Guar gum and its composites as potential materials for diverse applications: A review," *Carbohydrate Polymers*, vol. 199, no. -, pp. 534-545, Nov. 2018, doi: <https://doi.org/10.1016/j.carbpol.2018.07.053>
- [13] S. Rahman, A. Konwar, G. Majumdar, and D. Chowdhury, "Guar gum-chitosan composite film as excellent material for packaging application," *Carbohydrate Polymer Technologies and Applications*, vol. 2, p. 100158, Dec. 2021, doi: <https://doi.org/10.1016/j.carpta.2021.100158>.
- [14] F. Hong et al., "Chitosan-based hydrogels: From preparation to applications, a review," *Food Chemistry: X*, vol. 21, p. 101095, Mar. 2024, doi: <https://doi.org/10.1016/j.fochx.2023.101095>.
- [15] M. Barman et al., "Banana fibre-chitosan-guar gum composite as an alternative wound healing material," *International Journal of Biological Macromolecules*, vol. 259, pp. 129653-129653, Feb. 2024, doi: <https://doi.org/10.1016/j.ijbiomac.2024.129653>.
- [16] A. S. Amarasekara, D. Wang, and T. L. Grady, "A comparison of kombucha SCOBY bacterial cellulose purification methods," *SN Applied Sciences*, vol. 2, no. 240, pp. 1-7, Jan. 2020, doi: <https://doi.org/10.1007/s42452-020-1982-2>.
- [17] T. Tran et al., "Shedding Light on the Formation and Structure of Kombucha Biofilm Using Two-Photon Fluorescence Microscopy," *Frontiers in Microbiology*, vol. 12, Aug. 2021, doi: <https://doi.org/10.3389/fmicb.2021.725379>.
- [18] D. A. Safta, C. Bogdan, S. Iurian, and M.-L. Moldovan, "Optimization of Film-Dressings

- Containing Herbal Extracts for Wound Care—A Quality by Design Approach,” *Gels*, vol. 11, no. 5, p. 322, Apr. 2025, doi: <https://doi.org/10.3390/gels11050322>.
- [19] F. Daus, D. Montroni, L. Pesavento, M. Bruschi, A. Liguori, and M. L. Focarete, “Influence of the thickness of Symbiotic Culture of Bacteria and Yeast on purification and final properties of bacterial cellulose,” *Carbohydrate Polymer Technologies and Applications*, vol. 9, no. 2, pp. 100645–100645, Dec. 2024, doi: <https://doi.org/10.1016/j.carpta.2024.100645>.
- [20] A. Q. Chong, N. L. Chin, R. A. Talib, and R. K. Basha, “Modelling pH Dynamics, SCOBY Biomass Formation, and Acetic Acid Production of Kombucha Fermentation Using Black, Green, and Oolong Teas,” *Processes*, vol. 12, no. 7, pp. 1301–1301, Jun. 2024, doi: <https://doi.org/10.3390/pr12071301>.
- [21] M. Chen et al., “Hydrogen bonding impact on chitosan plasticization,” *Carbohydrate Polymers*, vol. 200, no., pp. 115–121, Nov. 2018, doi: <https://doi.org/10.1016/j.carbpol.2018.07.062>.
- [22] J. S. Mervis, “The Impact of Chronic Wound Exudate on the Patient, Clinician and Payer: Addressing the Challenges With Foam Dressings,” *International Wound Journal*, vol. 22, no. S1, Apr. 2025, doi: <https://doi.org/10.1111/iwj.70369>.
- [23] A. Tshikovhi, S. B. Mishra, A. K. Mishra, M. J. Mochane, and T. E. Motaung, “Efficient Removal of Mercury Ions Stabilized by Gold Solution Using Chitosan–Guar Gum Polymer Blend in Basic Media,” *Polymers*, vol. 17, no. 7, p. 985, Apr. 2025, doi: <https://doi.org/10.3390/polym17070985>.
- [24] Aneeqa Zarbab, A. Sajjad, A. Rasul, F. Jabeen, and M. J. Iqbal, “Synthesis and characterization of Guar gum based biopolymeric hydrogels as carrier materials for controlled delivery of methotrexate to treat colon cancer,” *Saudi Journal of Biological Sciences*, vol. 30, no. 8, pp. 103731–103731, Jul. 2023, doi: <https://doi.org/10.1016/j.sjbs.2023.103731>.
- [25] R. Dang, J. Xu, B. Zhang, S. Zhao, and Y. Dang, “Preparation of bacterial cellulose-based antimicrobial materials and their applications in wound dressing: A review,” *Materials & Design*, vol. 253, no. - p. 113820, Mar. 2025, doi: <https://doi.org/10.1016/j.matdes.2025.113820>.
- [26] C. Ardean et al., “Factors Influencing the Antibacterial Activity of Chitosan and Chitosan Modified by Functionalization,” *International Journal of Molecular Sciences*, vol. 22, no. 14, p. 7449, Jul. 2021, doi: <https://doi.org/10.3390/ijms22147449>.
- [27] C.-L. Ke, F.-S. Deng, C.-Y. Chuang, and C.-H. Lin, “Antimicrobial Actions and Applications of Chitosan,” *Polymers*, vol. 13, no. 6, p. 904, Mar. 2021, doi: <https://doi.org/10.3390/polym13060904>.
- [28] M. S. Rao, S. R. Kanatt, S. P. Chawla, and A. Sharma, “Chitosan and guar gum composite films: Preparation, physical, mechanical and antimicrobial properties,” *Carbohydrate Polymers*, vol. 82, no. 4, pp. 1243–1247, Nov. 2010, doi: <https://doi.org/10.1016/j.carbpol.2010.06.058>